New Journal of Physics
The open-access journal for physics

Resonant heating and substrate-mediated cooling of a single C_{60} molecule in a tunnel junction

Gunnar Schulze, Katharina J Franke and Jose Ignacio Pascual[1]
Institut für Experimentalphysik, Freie Universität Berlin, Arnimallee 14, 14195 Berlin, Germany
E-mail: pascual@physik.fu-berlin.de

New Journal of Physics **10** (2008) 065005 (11pp)
Received 8 February 2008
Published 30 June 2008
Online at http://www.njp.org/
doi:10.1088/1367-2630/10/6/065005

Abstract. We study the influence of different metallic substrates on the electron-induced heating and heat dissipation of single C_{60} molecules in the junction of a low temperature scanning tunneling microscope. The electron current passing through the molecule produces a large amount of heat due to electron–phonon coupling, eventually leading to thermal decomposition of the fullerene cage. The power for decomposition varies with electron energy and reflects the resonance structure participating in the transport. The average value for thermal decomposition of C_{60} on Cu(110) is 21 μW, whereas it is much lower on Pb(111) (2.9 μW) and Au(111) (1.0 μW). We ascribe this difference to the amount of charge transfer into C_{60} upon adsorption on the different surfaces, which facilitates molecular vibron quenching by electron–hole pair creation.

Contents

[1] Author to whom any correspondence should be addressed.

1. Introduction

A single molecule junction that is exposed to the flow of an electron current will experience an increase of temperature due to the heat generated by conduction electrons. Recent theoretical studies predicted that Joule heating in molecular junctions can be large enough to affect the reliability of molecular devices [1]. The temperature of a molecular junction is difficult to estimate. Recent experimental approaches have found agreement in that a single molecule device can easily reach several hundreds of degrees under normal operation (flow of microwatts when powered with 1 V) [2]–[5]. For most molecules, such a temperature reaches the limit of thermal degradation. Therefore, a deeper knowledge of the microscopic mechanisms of heat generation and dissipation on the nanoscale is required in order to improve the performance of a molecular device.

The temperature at the junction is a consequence of the equilibrium between heating and dissipation of heat away from the molecule. Heat generation is essentially caused by scattering of electrons with molecular vibrations. Heat dissipation is expected to follow several mechanisms involved in the coupling of the hot molecule with the substrate acting as an external cold bath. According to this, the temperature reached by a single molecule during electron transport should depend on the lead's material. Furthermore, one would expect that both the phonon bandwidth and the electronic density of states (DOS) around the Fermi energy should govern *a priori* the mechanisms of heat dissipation (cooling) and, hence, the molecular temperature.

In this paper, we analyze the effect of the lead's material on the heat dissipated during electron transport through a single molecule. We use a low temperature scanning tunneling microscope (STM) to inject an electron current through a single fullerene adsorbed onto clean metal surfaces of different nature. Rather than measuring the temperature reached by the single molecule, we follow the approach described in our previous work [5]. We look for certain current and sample bias (V_s) values at which the molecule under the STM tip undergoes an irreversible thermal degradation. The applied power required to reach the decomposition limit (P_{dec}) varies slightly with the electron energy (eV_s) in a sequence that resembles the energy alignment of the fullerene resonances for every metal substrate, confirming a resonant mechanism of electron heating [6]. However, we also find that the mean values of P_{dec} ($\bar{P}_{dec}$) depend more strongly on the substrate onto which the fullerenes are adsorbed. The way that $\bar{P}_{dec}$ scales for different metals cannot be explained in terms of the intrinsic properties of each material. Instead, the observed trend seems to be a result of the mechanism of interaction between the metal and the molecule. In particular, we find a correlation between the behavior of $\bar{P}_{dec}$ and the amount of charge transfer into molecular unoccupied states, as resolved using local spectroscopy measurements of C_{60} molecules on the different substrates. Hence, our results suggest that charge transfer processes at the metal–molecule contact provide an effective pathway to dissipate heat from a hot molecule through the creation of electron–hole (e–h) pairs.

2. Adsorption of C_{60} on Cu(110), Pb(111) and Au(111)

The experiments were performed in a custom-made ultra-high vacuum STM, which is operated at a temperature of 5 K. We chose Cu(110), Pb(111) and Au(111) single crystals as substrates because of their different properties regarding chemical reactivity, as well as phonon bandwidths and DOS at the Fermi energy (E_F). Cleaning of the metal substrates was performed by standard

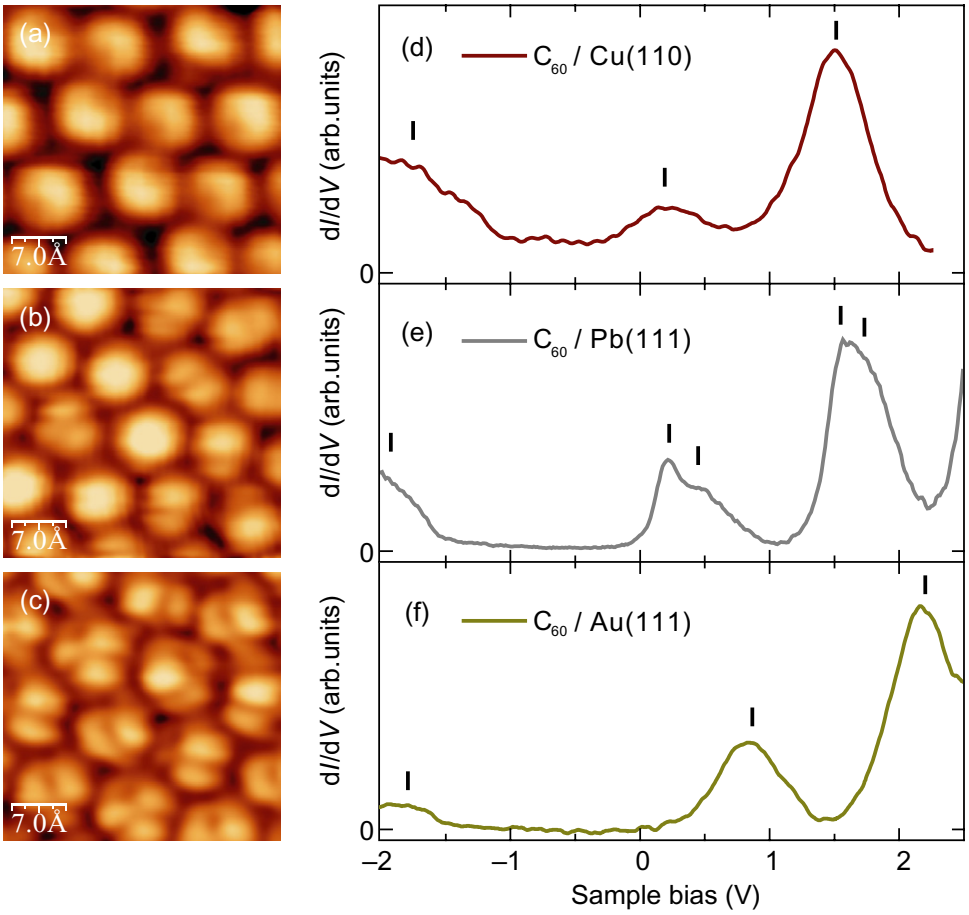

Figure 1. (a)–(c) STM images of C_{60} islands on Cu(110) ($I_t = 1.0$ nA, $V_s = 2.25$ V), Pb(111) ($I_t = 2.0$ nA, $V_s = 0.5$ V) and Au(111) ($I_t = 0.6$ nA, $V_s = 0.4$ V). (d) and (e) The corresponding tunnel conductivity spectra (dI/dV_s) of C_{60} on the different surfaces. Bars mark the fitted positions of HOMO, LUMO and LUMO + 1. Two peaks were fitted to the LUMO and LUMO + 1 levels on Pb(111). The spectra were measured by positioning the STM tip on top of a single molecule and ramping V_s while keeping the tip–molecule distance constant (feedback-loop open). dI/dV_s data were obtained by using a lock-in amplifier with an rms modulation amplitude V_{ac}. (Cu: $R_{junct} = 1.1$ GΩ, $V_{ac} = 20$ mV, Pb: $R_{junct} = 0.7$ GΩ, $V_{ac} = 5$ mV, Au: $R_{junct} = 0.3$ GΩ, $V_{ac} = 30$ mV.)

sputtering–annealing cycles under ultra-high vacuum, ensuring an atomically clean and flat metal surface. Indentations of the STM tip into the substrate while applying a tip–sample bias were used to clean the tips at regular intervals. The tips are therefore believed to be composed of the same material as the substrate. A sub-monolayer coverage of C_{60} molecules was deposited from a Knudsen cell on the metal surfaces at room temperature. On Cu(110) the system was further annealed to 470 K to ensure that the molecules self-assemble in ordered domains and populate a thermally stable adsorption state. The structure and electronic configuration of the molecular layers were characterized using STM and scanning tunneling spectroscopy (STS) measurements (figure 1).

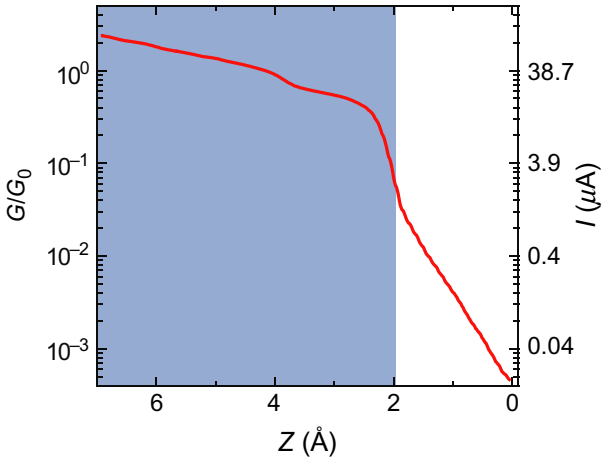

Figure 2. Conductance and current versus Z-distance plot $I(Z)$ on the top of a C_{60} molecule on Cu(110) ($V_s = 0.5$ V). The blue shaded area indicates the contact regime.

On Cu(110), C_{60} forms ordered islands with a pseudo-hexagonal structure (figure 1(a)), in which the fullerenes adopt a well-defined adsorption configuration with a pentagon–hexagon C–C bond pointing upwards [5, 7]. An STS spectrum on these molecules (figure 1(d)) resolves a clear spectroscopic fingerprint characterized by a sharp resonance at ∼1.5 eV above the Fermi level and associated with the alignment of the LUMO + 1 resonance (LUMO: lowest unoccupied molecular orbital). The LUMO resonance appears as a broader peak centered at ∼0.2 eV and is partially occupied.

Fullerene adsorption on Pb(111) at room temperature results in highly ordered hexagonal islands (figure 1(b)). Here, STS reveals the LUMO and LUMO + 1 derived resonances as in Cu(110) but more pronounced and with a characteristic split structure due to the breaking of degeneracy upon adsorption[2] (figure 1(e)). The energetic alignment of the LUMO close to E_F, with a small tail crossing it, indicates a small amount of charge transfer into C_{60}.

C_{60} islands on Au(111) evidence a similar hexagonal lattice as on Pb(111) (figure 1(c)), but with a large variety regarding molecular orientations [9], as one can determine from the intramolecular structure resembling the lobed shape of the LUMO resonance [10]. Both LUMO and LUMO + 1 resonances are resolved in STS spectra as pronounced peaks, independently of the molecular orientation [11]. The LUMO peak appears to be located far from E_F, at ∼0.8 eV, thus indicating that charge transfer from the substrate is very small [12].

3. C_{60} decomposition on metal surfaces

In our experiment, we approach the STM tip a distance Z towards a single C_{60} molecule while holding the sample bias V_s constant. During approach we record the current flowing through the molecular junction ($I(Z)$) (figure 2). The tunnel regime is revealed by an exponential increase of $I(Z)$ with diminishing gap distance. At a certain approach distance the $I(Z)$ curves deviate smoothly from the exponential dependence, indicating the onset of a tip–molecule contact [3]. The conductivity at this point is a small fraction of G_0 ($G_0 = 77.5\,\mu$S). For small positive

[2] Such a split structure can also be observed on other substrates but depends on the molecular orientation (e.g. [8]).

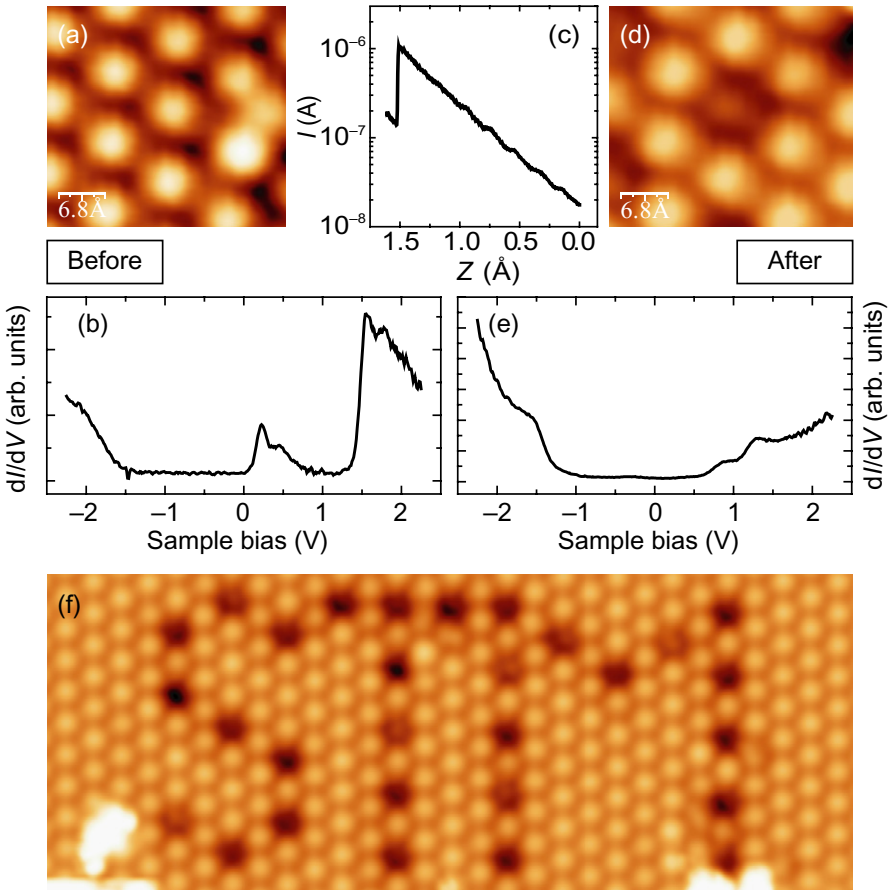

Figure 3. Molecular decomposition of C_{60} on a Pb(111) surface. (a) and (b) STM image and dI/dV_s plot of an intact C_{60} (central molecule). (c) Typical $I(Z)$ curve of a tip approach experiment showing one decomposition event in the tunneling regime ($V_s = 2.75$ V). (d) and (e) STM image and dI/dV_s plot of the molecule from (a) and (b) after decomposition events on the central molecule and on molecules at the image border. A height difference of 0.7 Å and the disappearance of the characteristic LUMO and LUMO + 1 resonances confirm the degradation of the C_{60} molecule. (a) $I_t = 0.2$ nA, $V_s = 0.5$ V, (d) $I_t = 0.2$ nA, $V_s = 2.25$ V, (b) and (e) $R_{junc} = 2.3$ GΩ; (f) image of the letters 'STM' created by successive decomposition events, to illustrate the high reproducibility ($I_t = 0.2$ nA, $V_s = 0.5$ V).

sample bias, the molecule remains intact upon contact formation and even further indentations of several Ångstroms, leading to a stable junction with the molecule contacted by the STM tip, on the one side, and the metal surface, on the other [3, 5]. In this case, the integrity of the indented molecule after tip contact can be verified by its appearance in the STM images and especially by its electronic fingerprint in dI/dV_s spectra.

Figure 3 shows, for the case of Pb(111), the effect of approaching a molecule at bias voltages above a threshold value of $V_s = 1.0$ V. A sharp drop appears in the $I(Z)$ curves

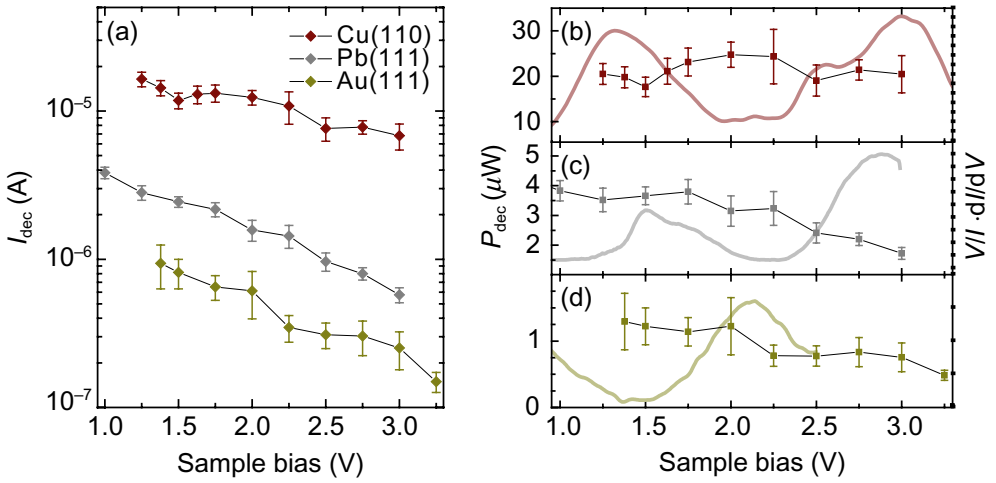

Figure 4. (a) Statistical average of decomposition currents $I_{dec}(V_s)$ in the tunneling regime for the three different surfaces. The total numbers of recorded events are: 152 on Cu(110), 150 on Pb(111) and 105 on Au(111). (b)–(d) Statistical average of the decomposition power $P_{dec}(V_s)$ for (b) Cu(110), (c) Pb(111) and (d) Au(111). The 2σ error bars are indicated in all figures. Normalized dI/dV spectra of C_{60} on the different substrates are added as shaded curves for comparison (Cu: $R_{junc} = 0.9\,G\Omega$, Pb: $R_{junc} = 0.7\,G\Omega$, Au: $R_{junc} = 0.3\,G\Omega$).

before reaching the contact regime[3], denoting the occurrence of an irreversible change in the junction (figure 3(c)). Similar results can also be found on Cu(110) for $V_s > 1.2\,V$ [5] and on Au(111) for $V_s > 1.5\,V$. After this current drop, STM images reveal that the molecule is transformed into a lower feature (figure 3(d)) and the characteristic resonances of the fullerene icosahedral cavity are absent from its corresponding STS spectrum (figure 3(e)). Hence, the discontinuous current drop is a fingerprint of degradation of the fullerene cage. The precise way in which the C_{60} decomposes cannot be determined in detail in our measurements. The effect is observed solely on the molecule selected for the tip approach and shows a high reproducibility, as depicted in figure 3(f) for the case of C_{60} on Pb(111) and, as shown in [5], on Cu(110).[4] A mechanical breaking of the fullerene cage can be excluded since the process takes place before a tip–molecule contact is formed (i.e. in the tunneling regime). We can then conclude that the decomposition is a current-induced thermal process.

The current I_{dec} at which the C_{60} decomposition occurs can be taken from the $I(Z)$ approach curves. I_{dec} turns out to show very reproducible values distinctive for every metal substrate and a clear dependence on the bias voltage used during the tip approach. Figure 4

[3] Below this threshold bias a discontinuity associated with C_{60} degradation is still found, but once the tip–molecule contact has been formed. Below $V_s = 0.6\,eV$ for Cu(110), $V_s = 0.6\,eV$ for Pb(111) and $V_s = 1.1\,eV$ for Au(111)) the C_{60} molecules remained intact [5].

[4] It should be noted that decomposition is not the only possible process observed during the tip approach. Especially rotations of the molecular orientation are known from other surfaces [13] and can often be found on Au(111). These events exhibit a similar tunnel current drop behavior as the decompositions do. They can be identified by inspection of the dI/dV_s spectra (no serious changes in the resonances are observed in these cases) and have to be excluded from the statistics.

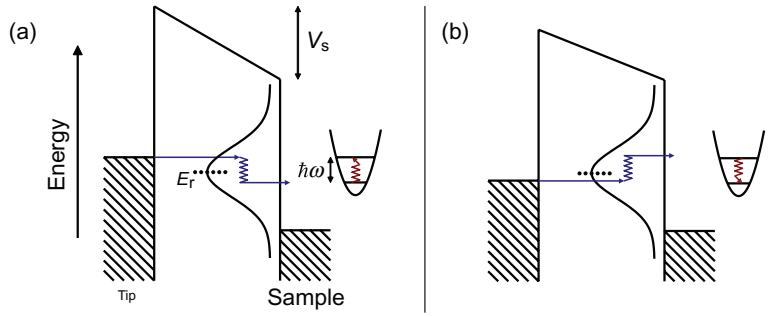

Figure 5. Schematic drawings of vibron interactions with tunneling electrons for a molecule inside a tunnel junction: (a) inelastic electron–vibron scattering at a resonance level E_r heats the molecule; (b) vibron-assisted tunneling is a cooling effect most effective for electron energies close to and below E_r.

shows the statistical average of I_{dec} plotted versus V_s for all three surfaces. Adsorbed on Cu(110), C_{60} molecules can withstand currents of several tens of microamperes, typically one order of magnitude larger than for C_{60} on Pb(111) or Au(111). In general, I_{dec} decreases monotonically as the applied bias is increased. Additionally, some faint steps can be inferred. This substructure becomes more evident when we plot instead the applied power necessary to decompose the molecule, $P_{dec} = V_s \times I_{dec}$ (figures 4(b)–(d)).

The monotonic decrease of I_{dec} transforms in a fairly flat behavior of P_{dec} with the applied bias. Figures 4(b)–(d) show that the average power applied for degradation depends strongly on the substrate used: $\bar{P}_{dec} \sim 21\,\mu$W for Cu(110), $\bar{P}_{dec} \sim 2.9\,\mu$W for Pb(111), and $\bar{P}_{dec} \sim 1\,\mu$W for Au(111). Superimposed on these values, the stepped substructure appears now more pronounced. The structure is correlated with the alignment of the unoccupied states of the C_{60} molecule, also shown in figure 4(b)–(d). In general, we find that P_{dec} decreases whenever a new resonance (here the LUMO + 1 and LUMO + 2) enters the conduction energy window. Hence, the molecular resonance structure is reflected in the power needed to decompose a molecule. Next, we interpret the origin of this resonant substructure (section 4) and of the strong substrate dependence of the applied power for degradation $\bar{P}_{dec}$ (section 5).

4. Molecular heating and cooling mechanisms

The origin of the substructure in the P_{dec} versus V_s plots can be understood from current theoretical models describing the electron-induced heating of single molecules during electron transport [14, 15]. Heat inside the molecule is generated by inelastic scattering of tunneling electrons with molecular vibrations (figure 5(a)). For the large tunneling rates used in our experiment, electron scattering leads to a non-equilibrium distribution of excited modes, whose internal energy can be associated with a molecular temperature T_m. For a certain set of current and bias values, T_m depends on the balance between the *heat generated* by the inelastic scattering of electrons with molecular modes and *heat dissipated* into the 'cold' electrode, in our experiment at 5 K [6, 14, 16].

Recent calculations [6] have shown that when a new resonance level E_r enters the transport energy window (hence, when $eV_s > E_r$), a steep temperature increase takes place in the molecule as a consequence of more vibronic levels being accessible (figure 5(a)). Hence,

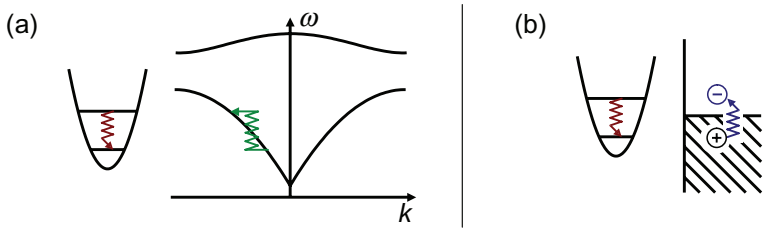

Figure 6. Schematic drawings of mechanisms of molecular vibration decay into excitations of the cold metal substrate: (a) decay into the metal phonon band and (b) creation of excited metal electrons (e–h pairs) close to the Fermi edge are substrate-dependent cooling effects.

the increase in temperature upon crossing a resonance level manifests itself as a step-like decrease of the corresponding decomposition current I_{dec} and power P_{dec}, as shown in the plots of figure 4.

In contrast to this, tunnel electrons can also absorb vibrons of a hot molecule (figure 5(b)), leading to reduced heat generation. When the sample bias lies right below a resonance level $eV_s \leqslant E_r$, this cooling mechanism can be very effective and eventually causes a lower rise of molecular temperature with V_s [5]. This behavior translates into plateaus in I_{dec} and increase in P_{dec} at bias values below the corresponding resonance energy.

Qualitatively, the combination of both heating and cooling processes accounts well for the correspondence between the stepped (oscillating) behavior of the $I_{dec}(P_{dec})$ plots and the resonant structure of the molecule in figure 4.[5] However, it cannot explain the striking differences in $\bar{P}_{dec}$ found for the different substrates. Since the mechanisms of heating/cooling by tunneling electrons depend on the coupling between tunnel electrons and molecular vibrons, they are not expected to vary much on the different substrates. Hence, the large differences in $\bar{P}_{dec}$ must be related to substrate-mediated mechanisms of cooling the molecule.

5. Substrate dependence of decomposition power

Further mechanisms of molecular cooling are those in which molecular hot modes decay by creating quasiparticle excitations in the substrate (either e–h pairs or phonons). In agreement with our findings, these excitations do not depend on the sample bias but may vary depending on the substrate's electronic and phononic properties.

Decay of molecular vibrons into substrate phonons plays a minor role in cooling the molecule, since this mechanism is limited by the phonon bandwidth of the substrates (figure 6(a)). The Cu(110) phonon band is approximately 42 meV wide and therefore larger than in Pb(111) (14 meV [17]) and in Au(111) (16 meV [18]). However, the 174 internal modes of C_{60} have energies between 33 and 200 meV. Hence, substrate phonons are expected to be primarily coupled to external molecular vibrations of the C_{60} molecule with respect to the surface, which do not contribute to the thermal decomposition of the fullerene cage.

The most important contribution to the observed substrate dependence of $\bar{P}_{dec}$ is the varying efficiencies of molecular cooling through e–h pair creation (figure 6(b)) [19]. Since the

[5] On Pb(111), the LUMO + 1 resonance is found to be split into two peaks at 1.5 and 1.8 V. The position of the P_{dec} step at 1.8 V on Pb in figure 4 is probably due to the high energetic component of this resonance.

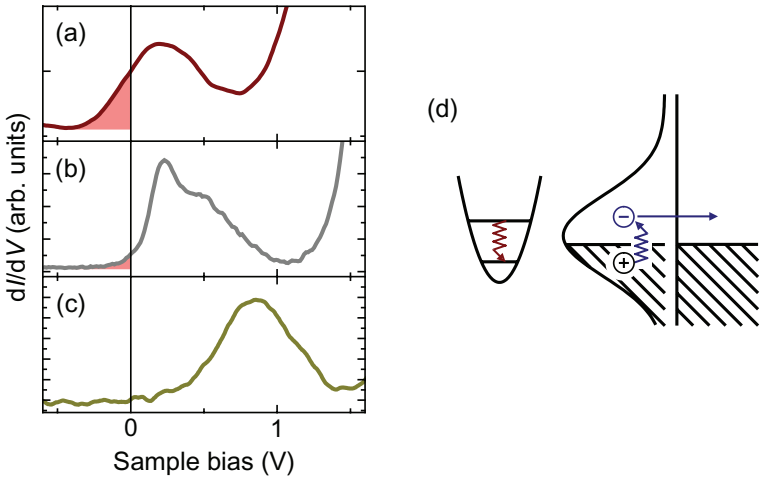

Figure 7. (a)–(c) Magnification of the dI/dV_s curves of figures 1(d)–(f) showing the LUMO of C_{60} on (a) Cu(110), (b) Pb(111) and (c) Au(111). The occupied portions of the LUMO peaks are marked as shaded areas. From this a decreasing amount of electron transfer into the molecule can be expected for Cu(110) to Pb(111) to Au(111). (d) Schematic drawing of the proposed mechanism of vibron decay by e–h pair creation in a partially occupied molecular resonance. The large spatial overlap of the molecule and metal states at E_F increases the decay probability. The e–h pairs excited inside the molecule can leave before they recombine.

final states lie at excitation energies in the order of the vibrational bandwidth of the molecule, the decay rate scales with the DOS around E_F. On Cu(110) and Au(111), surface states provide most of the available states in this energy region, according to available data on DOS at E_F.[6] It can therefore be expected that e–h pair creation is favored on Cu(110) with respect to the gold surface, in agreement with our observations. However, this mechanism fails to explain the intermediate $\bar{P}_{dec}$ value found for degradation of C_{60} on Pb(111), since this metal surface has no surface state, and its density of bulk states at E_F is also the lowest of all three metals (see footnote 6).

To solve this puzzle we note that the absorption of molecular vibrons through excitation of e–h pairs rather depends on the DOS around E_F in the C_{60} molecule coming from the surface [5, 24]. Therefore, this dissipation channel should not be viewed as an intrinsic property of the substrate material, but as a consequence of the molecule–surface interaction. In our case, we could experimentally determine that the LUMO derived resonances of C_{60} on different metals exhibit a different degree of weight at the Fermi energy, associated with different amounts of charge transfer from the surface. In fact, the degree of charge transfer (increasing from Au(111) over Pb(111) to Cu(110), as shown in figures 7(a)–(c)) follows the trend found for $\bar{P}_{dec}$ in figure 4.

[6] Density of surface states are approximately 0.017 and 0.0105 $(eV\,Å^2)^{-1}$, for Cu(110) and Au(111), respectively [20]–[22]. The bulk DOS at E_F is: $DOS_{Pb}(E_F) = 0.0166\,(eV\,Å^3)^{-1}$, $DOS_{Au}(E_F) = 0.0173\,(eV\,Å^3)^{-1}$ and $DOS_{Cu}(E_F) = 0.025\,(eV\,Å^3)^{-1}$ [23].

This allows us to depict a qualitative picture, in which charge transfer from the metal causes an increase of the density of molecular states around E_F. This favors the generation of e–h pairs at the molecule, which are then reflected back into the metal where they recombine. The rate of heat dissipation thus increases with the charge transfer, causing the requirement for a larger power to thermally degrade the single molecule. Ignoring additional mechanisms and effects like hybridization of metal and molecule states, which probably could also play an important role here, our results hint that charging a single molecule in contact with a metal electrode can help to sustain larger current densities crossing through a single molecule.

6. Summary

Our experiments reveal that electronic currents in the range of 0.1–20 μA and powers in the order of 1–30 μW are sufficient to generate heat in single C_{60} molecules leading to thermal decomposition on metal surfaces. The decomposition power results from the balance of molecular heating and cooling. While the former is substrate-independent, the latter varies on the different substrates as a function of charge transfer into the molecule. Charge transfer assures an effective quenching of molecular vibrons into e–h pairs. In order to increase the current density a molecular junction can sustain, it is desirable to choose a substrate where molecular adsorption leads to a partial filling of molecular states by substrate electrons.

Acknowledgments

We thank Alessio Gagliardi and Alessandro Pecchia for helpful discussions. This research was supported by the Deutsche Forschungsgemeinschaft through the collaborative projects SPP 1243 and Sfb 658.

References

[1] Galperin M, Ratner M A and Nitzan A 2007 *J. Phys: Condens. Matter* **19** 103201
[2] Huang Z, Xu B, Chen Y, Di Ventra M and Tao N 2006 *Nano Lett.* **6** 1240
[3] Néel N, Kröger J, Limot L, Frederiksen T, Brandbyge M and Berndt R 2007 *Phys. Rev. Lett.* **98** 065502
[4] Huang Z, Chen F, D'agosta R, Bennett P A, Di Ventra M and Tao N 2007 *Nat. Nanotechnol.* **2** 698
[5] Schulze G *et al* 2008 *Phys. Rev. Lett.* **100** 136801
[6] Pecchia A, Romano G and Di Carlo A 2007 *Phys. Rev.* B **75** 035401
[7] Fasel R, Agostino R G, Aebi P and Schlapbach L 1999 *Phys. Rev.* B **60** 4517
[8] Franke K J, Schulze G, Henningsen N, Fernández-Torrente I, Pascual J I, Zarwell S, Rück-Braun K, Cobian M and Lorente N 2008 *Phys. Rev. Lett.* **100** 036807
[9] Schull G and Berndt R 2007 *Phys. Rev. Lett.* **99** 226105
[10] Pascual J I, Gomez-Herrero J, Sanchez-Portal D and Rust H-P 2002 *J. Chem. Phys.* **117** 9531
[11] Rogero C, Pascual J I, Gomez-Herrero J and Baro A M 2002 *J. Chem. Phys.* **116** 832
[12] Lu X, Grobis M, Khoo K H, Louie S G and Crommie M F 2004 *Phys. Rev.* B **70** 115418
[13] Néel N, Kröger J, Limot L, Frederiksen T, Brandbyge M and Berndt R 2007 Rotation of C_{60} in a single-molecule contact *Preprint* 0710.1417
[14] Galperin M, Ratner M A and Nitzan A 2007 *J. Phys.: Condens. Matter* **19** 103201
[15] Galperin M, Nitzan A and Ratner M A 2007 *Phys. Rev.* B **75** 155312
[16] Romano G, Pecchia A and Di Carlo A 2007 *J. Phys.: Condens. Matter* **19** 215207
[17] Fuhrmann D and Wöll C 1996 *Surf. Sci.* **368** 20–6

[18] Wang X Q 1991 *Phys. Rev. Lett.* **67** 1294–7
[19] Gao S, Persson M and Lundqvist B I 1992 *Solid State Commun.* **84** 271
[20] Kevan S 1983 *Phys. Rev.* B **28** 4822–4
[21] Aebi P, Osterwalder J, Fasel R, Naumović D and Schlapbach L 1994 *Surf. Sci.* **307–309** 917–21
[22] LaShell S, McDougall B A and Jensen E 1996 *Phys. Rev. Lett.* **77** 3419–22
[23] Papaconstantopoulos D A 1986 *Handbook of the Band Structure of Elemental Solids* (New York: Plenum)
[24] Gagliardi A, private communication